Anal. Chem. **2005,** *77,* 1096−1105

Stable and Functional Immobilization of Histidine-Tagged Proteins via Multivalent Chelator Headgroups on a Molecular Poly(ethylene glycol) Brush

Suman Lata and Jacob Piehler*

Institute of Biochemistry, Johann Wolfgang Goethe-University, Marie-Curie-Strasse 9, 60439 Frankfurt am Main, Germany

We present a generic approach for immobilizing oligohistidine-tagged proteins with high stability and homogeneous functionality onto glass-type surfaces. Multivalent chelator heads (MCH) carrying two and three nitrilotriacetic acid (NTA) moieties were coupled with controlled surface concentration to glass surfaces premodified with an ultrathin two-dimensional polymer brush of a bifunctional poly(ethylene glycol). Low roughness and lateral homogeneity of these surfaces were confirmed by AFM and fluorescence microscopy, respectively. Protein immobilization and interactions at these interfaces were studied by label-free and fluorescence detection. Oligohistidine-tagged proteins bound specifically to NTA loaded with nickel(II) ions and could be eluted with imidazole. More than 90% of the immobilized protein preserved its activity. In contrast to mono-NTA, immobilized multivalent chelator heads bound oligohistidine-tagged proteins stoichiometrically and with high stability, even at very low chelator surface concentrations. Thus, an excess of the metal chelator sites was not necessary, and excessive binding sites could be quantitatively blocked with an indifferent protein. As a consequence, increased functional stability of the immobilized protein and a substantial reduction in nonspecific adsorption were achieved. Binding of histidine-tagged proteins to the MCH-modified surface was efficiently blocked by stoichiometric amounts of soluble MCH, and biomolecular interaction unbiased by the interaction of the histidine tag to the surface-bound MCH was observed. These excellent features and the compatibility with many solid-phase analytical techniques make this surface chemistry beneficial for functional protein analysis.

Modern proteomic research increasingly demands analytical techniques for studying protein actions in highly multiplexed assay formats. The development of generic analytical tools for functional proteomics is challenging due to the fragile and varied nature of proteins. Solid-phase assay formats offer several distinct advantages: low sample consumption, simple and automatizable sample handling, and a huge potential for parallelization.[1] Numerous solid-phase detection techniques have been established for probing biomolecular interactions on surfaces[2,3] and have been successfully applied to functional proteomics,[4] as well as drug discovery.[5] Furthermore, surface-sensitive techniques with sensitivities down to the level of individual molecules are increasingly employed for functional protein analysis at surfaces.[6,7] However, preserving homogeneous functionality of the immobilized protein is one of the most critical tasks, as the enormous physicochemical diversity of proteins hampers the use of generic methods. The requirements for suitable protein immobilization for solid-phase detection are manifold: (i) efficient coupling of the detection technique with the substrate; (ii) low nonspecific protein interaction with the surface; (iii) stable, yet reversible tethering of the proteins while maintaining their functionality on the surface homogeneously. For shielding the substrate surface against nonspecific adsorption, modification with hydrophilic, inert polymers has proven suitable for many types of surfaces.[8] These layers must be very thin in order not to affect the signal transducing properties of the substrate and homogeneous accessibility of the immobilized proteins. For the attachment of the proteins to polymer-modified surfaces, numerous methods have been employed:[3,9,10] covalent immobilization through amine or thiol-reactive linkers,[7] as well as specific antibodies and other affinity-based techniques.[8] Affinity capturing provides not only oriented and homogeneous attachment but also the possibility to reversibly detach the protein and thus repeated use of the same surface. An affinity capturing system very frequently employed for protein purification is the interaction of oligohistidine-tagged proteins with metal ions immobilized via chelators such as iminodiacetic acid[11] or nitrilotriacetic acid (NTA).[12] Many further applications have been reported,[13] including

* Corresponding author. E-mail: j.piehler@em.uni-frankfurt.de. Phone: +49 (0)69 79829468. Fax: +49 (0)69 79829495..

(1) Zhu, H.; Snyder, M. *Curr. Opin. Chem. Biol.* **2003**, *7*, 55−63.
(2) Brecht, A.; Gauglitz, G. *Biosens. Bioelectron.* **1995**, *10*, 923−936.
(3) Cooper, M. A. *Anal.Bioanal. Chem.* **2003**, *377*, 834−842.
(4) Zhou, H.; Roy, S.; Schulman, H.; Natan, M. J. *Trends Biotechnol.* **2001**, *19*, S34−S39.
(5) Cooper, M. A. *Nat. Rev. Drug Discovery* **2002**, *1*, 515−528.
(6) Ishijima, A.; Yanagida, T. *Trends Biochem. Sci.* **2001**, *26*, 438−444.
(7) Hinterdorfer, P.; Schutz, G.; Kienberger, F.; Schindler, H. *J. Biotechnol.* **2001**, *82*, 25−35.
(8) Ratner, B. D. *Biosens. Bioelectron.* **1995**, *10*, 797−804.
(9) O'Shannessy, D. J.; Brigham-Burke, M.; Peck, K. *Anal.Biochem.* **1992**, *205*, 132−136.
(10) Elia, G.; Silacci, M.; Scheurer, S.; Scheuermann, J.; Neri, D. *Trends Biotechnol.* **2002**, *20*, S19−S22.

10.1021/ac048813j CCC: $30.25
Published on Web 01/11/2005

protein immobilization on planar surfaces, e.g., NTA-modified glass-type surfaces,[14] NTA-functionalized dextran hydrogels,[15] and NTA-terminated (alkyl) thiol SAMs,[16,17] as well as solid-supported lipid bilayers doped with NTA-lipids.[18,19] Chelator-based immobilization offers some distinct advantages over biochemical recognition elements such as antibodies or streptavidin: metal ion chelators are of low molecular weight, chemically very defined, generally very stable, and compatible with organic synthesis. Furthermore, the interaction with histidine-tagged proteins can be selectively switched off by metal ions, coordinating ligands, or metal chelators under mild conditions. However, while for some proteins stable immobilization on planar surfaces via chelated metal ions (CMI) was possible, in many cases, substantial dissociation was observed on the time scale of a few minutes.[20] We and others ascribe this to the fact that the interaction between an individual oligohistidine tag and an individual CMI is insufficient for stable tethering, while the apparent stable binding is attributed to multipoint attachment and rebinding.[15,20] This scenario is readily achieved by a high density of metal chelator sites in a polymer matrix, but much less efficient on a planar surface. Stability gain by such heterogeneous multivalency is not in line with (i) spatially defined attachment of proteins on ultraflat surfaces and (ii) precise control of surface concentrations by adjusting the density of recognition sites. Furthermore, a high excess of CMI leads to nonspecific binding mediated by metal-coordinating amino acid (Cys, Glu, Asp, Arg, Lys, His) and possibly also affects the immobilized proteins. Thus, chelator heads, which enable stable and stoichiometric immobilization of histidine-tagged proteins, would provide a considerable advancement toward organizing and studying recombinant proteins on surfaces on a molecularly defined level.

Here, we describe a bottom-up approach for the modification of glass-type surfaces with the following features: (i) an ultrathin, dense poly(ethylene glycol) (PEG) layer to shield the substrate surface against nonspecific adsorption; (ii) tag-specific, oriented immobilization of the protein in a two-dimensional arrangement to ensure homogeneous accessibility and functionality; (iii) multivalent chelator heads (MCH) engineered for stable, yet switchable attachment of the proteins with controlled surface coverage. The physicochemical properties of these surfaces as well as attachment, functionality, and removal of oligohistidine-tagged proteins were investigated by various surface-sensitive techniques. We demonstrate that this adjustable modification strategy provides powerful means for studying recombinant proteins on surfaces.

EXPERIMENTAL SECTION

Materials. Diamino poly(ethylene glycol) (DAPEG) with an average molecular mass of 2000 g/mol was purchased from RAPP Polymere (Tübingen, Germany). Oregon Green 488 (OG488) NHS active ester was purchased from Molecular Probes. IFNβ (formulated Rebif 22 and 44 μg) was obtained from Serono GmbH (Unterschleissheim, Germany). Common organic compounds and biochemicals were purchased either from Fluka or from Sigma. Protected amino acids were purchased from Bachem (Weil am Rhein, Germany). The vector pMAL-c2x and factor Xa were purchased from New England Biolabs.

Protein Biochemistry. IFNα2 and ^{mut}IFNα2 (a mutant with an increased affinity toward ifnar1-EC), as well as tagless ifnar2-EC and the variants carrying a C-terminal hexahistidine-tag (ifnar2-H6), a C-terminal decahistidine-tag (ifnar2-H10), and the corresponding I47A mutant (^{I47A}ifnar2-H10) were expressed in *Escherichia coli*, refolded from inclusion bodies, and purified as described before.[21] Maltose binding protein (MBP) with a C-terminal H10- and a H6-tag (MBP-H10 and MBP-H6, respectively) were cloned by inserting oligonucleotide linkers encoding for the respective oligohistidine tags into multiple cloning site of the vector pMal-c2x. The proteins MBP-H6 and MBP-H10 were expressed according to the manufacturer's instructions and were purified by immobilized metal ion affinity chromatography (IMAC) and size exclusion chromatography. The integrity of the histidine tag was checked by proteolytic digestion with factor Xa and analysis by MALDI-MS. Purified MBP-H10 was labeled with OG488 NHS active ester and further purified by IMAC and size exclusion chromatography. All purified proteins were more than 95% homogeneous and monomeric as detected by nonreducing SDS–PAGE and size exclusion chromatography.

Chelator Headgroups and Surface Chemistry. The NTA-based chelator heads were synthesized with the carboxyl groups of the NTA moiety protected as tertiary butyl esters as shown in Figure 1A. Synthetic details will be described in a forthcoming paper. Briefly, the amine-functionalized NTA head **1**, which has been described before,[22] was grafted onto a suitably protected glutamic acid scaffold to yield **2**. The carboxyl-functionalized NTA head (structure not shown) was reacted with 1,4,8,11-tetraazacyclotetradecane under stoichiometric control to attach three NTA heads. In the second step, the fourth imino group was reacted with succinic anhydride to yield **3** (Figure 1A). These three protected chelator heads (**1**–**3**) were used for coupling to the PEG layers (Figure 1B). Reflectance interference spectroscopy (RIfS) transducer slides and glass coverslips for microscopy were cleaned with 3 M NaOH followed by incubation in a freshly prepared mixture of one part 30% hydrogen peroxide and two parts concentrated sulfuric acid (caution, highly corrosive!). After rinsing with water and drying in a nitrogen stream, the surfaces were silanized with (3-glycidyloxypropyl)trimethoxysilane (GOPTS), and DAPEG (2000 g/mol) was reacted with the epoxy groups on

(11) Porath, J.; Carlsson, J.; Olsson, I.; Belfrage, G. *Nature* **1975**, *258*, 598–599.
(12) Hochuli, E.; Dobeli, H.; Schacher, A. *J. Chromatogr.* **1987**, *411*, 177–184.
(13) Ueda, E. K.; Gout, P. W.; Morganti, L. *J. Chromatogr., A* **2003**, *988*, 1–23.
(14) Schmid, E. L.; Keller, T. A.; Dienes, Z.; Vogel, H. *Anal.Chem.* **1997**, *69*, 1979–1985.
(15) Gershon, P. D.; Khilko, S. *J. Immunol. Methods* **1995**, *183*, 65–76.
(16) Sigal, G. B.; Bamdad, C.; Barberis, A.; Strominger, J.; Whitesides, G. M. *Anal. Chem.* **1996**, *68*, 490–497.
(17) Riener, C. K.; Kienberger, F.; Hahn, C. D.; Buchinger, G. M.; Egwim, I. O. C.; Haselgrubler, T.; Ebner, A.; Romanin, C.; Klampfl, C.; Lackner, B.; Prinz, H.; Blaas, D.; Hinterdorfer, P.; Gruber, H. J. *Anal. Chim. Acta* **2003**, *497*, 101–114.
(18) Dorn, I. T.; Pawlitschko, K.; Pettinger, S. C.; Tampe, R. *Biol. Chem.* **1998**, *379*, 1151–1159.
(19) Busch, K.; Tampe, R. *J. Biotechnol.* **2001**, *82*, 3–24.
(20) Nieba, L.; Nieba-Axmann, S. E.; Persson, A.; Hamalainen, M.; Edebratt, F.; Hansson, A.; Lidholm, J.; Magnusson, K.; Karlsson, A. F.; Pluckthun, A. *Anal. Biochem.* **1997**, *252*, 217–228.
(21) Piehler, J.; Schreiber, G. *J. Mol. Biol.* **1999**, *289*, 57–67.
(22) Dorn, I. T.; Neumaier, K. R.; Tampe, R. *J. Am. Chem. Soc.* **1998**, *120*, 2753–2763.

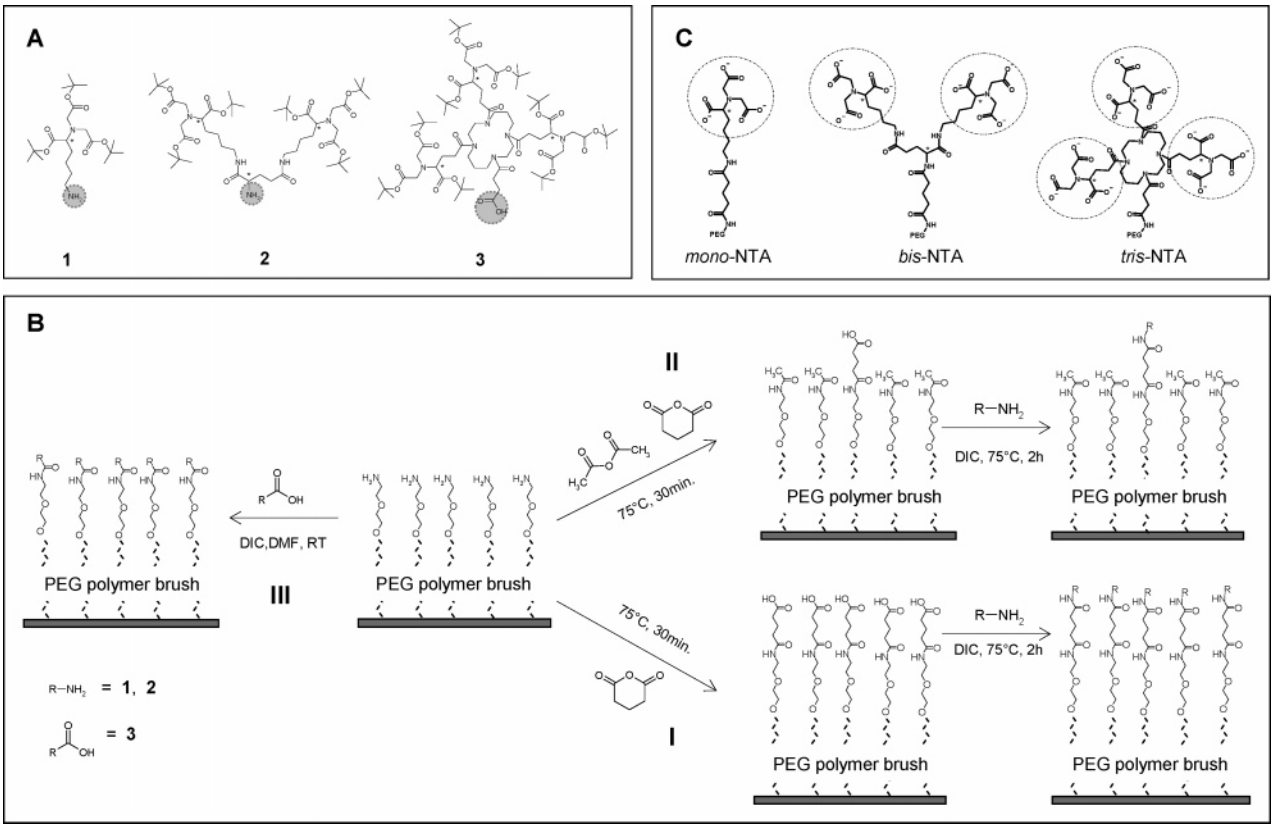

Figure 1. MCH and surface modification. (A) Chemical structures of the protected chelator heads, which were coupled to the surface. (B) Different pathways employed for coupling the chelator heads to the amine-functionalized PEG polymer brush: (I) coupling of mono- and bis-NTA in maximum surface concentrations; (II) coupling of mono- and bis-NTA in reduced surface concentrations; (III) coupling of tris-NTA. (C) Chemical structures of the immobilized MCH after deprotection on the surface (the NTA part is marked with dashed circles).

the surface as described before.[23] For coupling the amine-presenting chelator heads (**1**, **2**), the DAPEG layers were treated with molten glutaric anhydride at 75 °C for 20 min (Figure 1B, pathway I).[24] By diluting glutaric anhydride with acetic anhydride in different ratios, the carboxyl functionalization of the surface was systematically varied, and thus, the extent of chelator head functionalization was adjusted (Figure 1B, pathway II). The PEG layers treated with glutaric anhydride alone will be referred to as 100% functionalized layers, and the layers treated with 20 mol % glutaric anhydride will be referred to as 20% functionalized layers. After thoroughly rinsing with water and drying with nitrogen, 10 μL of the amine-presenting chelator heads in chloroform (100 mg/mL) was homogeneously applied onto the surface and the solvent was evaporated in a nitrogen stream. The coupling reaction was started by addition of 5 μL of DIC and subsequent incubation for 2 h at 75 °C by assembling the surfaces of two slides face to face. The carboxyl-presenting chelator headgroup **3** was directly coupled to untreated DAPEG layers (Figure 1B, pathway III). A mixture of 5 μL of **3** dissolved in DMF (100 mg/mL) with 5 μL of DIC was incubated on the DAPEG surfaces in a face-to-face assembly. The reaction was controlled by varying the reaction time between 2 min and 1 h. The excess reaction mixture was washed off with chloroform, and the transducers were incubated in neat TFA for 4 h to deprotect the chelator heads. The deprotected chelator heads carrying one, two, and three NTA moieties (Figure 1C) will be referred to as mono-, bis-, and tris-NTA, respectively.

Solid-Phase Detection. Protein immobilization and protein interactions were monitored label-free using RIfS. This technique detects binding on the surface of a thin silica interference layer.[25] A home-built setup based on a commercially available diode array spectrometer as described before[26] was used. Binding curves were obtained from the shift of the interference spectrum. A shift of 1 nm corresponds to ~1 ng/mm^2 protein on the surface.[27] Measurements were carried out in a flow chamber under continuous flow-through conditions with a data acquisition rate of 1 Hz as described before.[24]

Binding Assays. All binding assays were carried out with HBS (20 mM Hepes, pH 7.5, 150 mM NaCl, 0.01% Triton X100) as running buffer. Protein solutions were always prepared with the actual batch of the running buffer. The functionalized surfaces were treated with 100 mM HCl for 150 s followed by equilibration in HBS. The chelator heads were loaded with nickel(II) by injecting 30 mM nickel(II) chloride in HBS. Depending upon the targeted surface concentration, the oligohistidine-tagged proteins were injected at different concentrations (0.25−50 μM) for 150 or 400 s. For determining saturation binding signal R_{max}, oligo-

(23) Piehler, J.; Brecht, A.; Valiokas, R.; Liedberg, B.; Gauglitz, G. *Biosens. Bioelectron.* **2000**, *15*, 473−481.
(24) Piehler, J.; Schreiber, G. *Anal. Biochem.* **2001**, *289*, 173−186.
(25) Brecht, A.; Gauglitz, G.; Polster, J. *Biosens. Bioelectron.* **1993**, *8*, 387−392.
(26) Schmitt, H. M.; Brecht, A.; Piehler, J.; Gauglitz, G. *Biosens. Bioelectron.* **1997**, *12*, 809−816.
(27) Hanel, C.; Gauglitz, G. *Anal. Bioanal. Chem.* **2002**, *372*, 91−100.

histidine-tagged proteins were injected at a concentration of 50 μM for 150 s. The affinities of different multivalent chelator headgroups were assessed by imidazole-induced dissociation: oligohistidine-tagged proteins (300 nM) were injected on 100% functionalized surfaces for 400 s. The elution of the immobilized protein with different concentrations of imidazole (1−200 mM) was then monitored for 140 s. For assessing ligand binding to immobilized ifnar2-H10, IFNα2 (400 nM) or IFNβ (200 nM) were injected for 150 s, and the dissociation was monitored for 150−400 s. The immobilized proteins were removed by an injection of 150 mM imidazole, pH 7.5, for 150 s. The NTA-bound nickel(II) ions were removed by an injection of 50 mM EDTA pH 7.5.

Data Analysis. Binding curves were analyzed using BIAevaluation (Biacore AB, Uppsala, Sweden) and Origin (Microcal Software Inc., Northampton, MA). The mass-sensitive RIfS signal R directly reflects the amount of ligand bound to the surface. The dissociation phase of binding curves was fitted by different models. Ideally, the signal during the dissociation phase is given by

$$R = R_0 e^{-k_d(t-t_0)} \quad (1)$$

where k_d is the dissociation rate constant, R is the amount of bound ligand at time t, and R_0 is the amount of bound ligand at time t_0. At high surface concentration of unoccupied binding sites, the dissociated ligand can react with another binding site on the surface with a finite probability (rebinding).[28,29] Furthermore, redundancy of binding sites as provided by oligohistidine tags allows interaction with more than one site on the surface (multipoint attachment). For the imidazole-induced dissociation of histidine-tagged protein from chelator-modified surfaces, these effects were treated as binding to inhomogeneous binding sites and modeled by an arithmetic decrease of the apparent dissociation rate constant:

$$dR/dt = -[k_d - b(R_{max} - R)]R \quad (2)$$

where R_{max} is the saturation amplitude of the complex and b is the propensity for surface reactions occurring with between the bound ligand (R) and the free binding sites ($R_{max} - R$). The following solution satisfies the above stated differential equation:

$$R = \frac{R_{trapped}R_0}{(R_{trapped} - R_0)e^{-a\cdot(t-t_0)} + R_0} \quad (3)$$

with

$$a = bR_{max} - k_d \quad (3a)$$

and

$$R_{trapped} = R_{max} - k_d/b \quad (3b)$$

$R_{trapped}$ is the amount of bound protein, which remains on the surface when the dissociation rate equals zero, because it is "trapped" by rebinding. Equation 3 was fitted to the dissociation phase (corrected for the refractive index change due to imidazole in bulk) and $R_{trapped}$ was plotted as a function of imidazole concentration c. A logistic sigmoidal function

$$R_{trapped}(c) = \frac{R_{trapped,max}}{1 + (c/EC_{50})^p} \quad (4)$$

was fitted to these plots and EC_{50} and p were determined.

Confocal Laser Scanning Fluorescence Microscopy (CLSM). Fluorescence imaging was carried out with a laser scanning confocal microscope (LSM 510, Carl Zeiss Jena GmbH, Jena, Germany) equipped with a 25-mW argon ion laser. Protein immobilization was carried out in a flow cell with automated sample handling as described for RIfS. OG488-labeled MBP-H10 was first immobilized as described below and then imaged using 63× magnification objective by exciting at 488 nm with 0.1% laser power and scanning for 1.9 s. A round spot with a diameter of 25 μm was bleached by scanning for ~7 s at 100% laser power.

Atomic Force Microscopy (AFM). AFM measurements were carried out using a Multimode system equipped with a Nanoscope III controller (Digital Instruments Inc., Santa Barbara, CA). The modified transducer surfaces were incubated with 100 mM HCl for 3 min and then washed extensively with water. After drying, the transducers were mounted in the flow chamber and the flow chamber was filled with buffer (20 mM Hepes, 150 NaCl, pH 7.5). Cantilevers were oxide-sharpened silicon nitride tips (Digital Instruments) with a spring constant of 0.12 N/m. Imaging was typically performed in contact mode. In addition, tapping mode was employed to reduce distortion, but no significant differences were observed.

RESULTS AND DISCUSSION

The traditional mono-NTA as well as the novel multivalent chelator headgroups were coupled onto glass surfaces modified with a dense molecular PEG polymer brush. The binding of the oligohistidine-tagged proteins was then studied quantitatively in real time by label-free detection. Two different monomeric proteins with a single C-terminal oligohistidine tag were used: MBP and the extracellular domain of the type I interferon receptor subunit ifnar2 (ifnar2-EC). The biocompatibility of the surface was evaluated (i) by assessing the interferon α2 (IFNα2) binding activity of the immobilized H10-tagged ifnar2-EC (ifnar2-H10); (ii) and the nonspecific binding of a challenging analyte, namely, IFNβ. Important attributes of the immobilization strategy, e.g., reversibility and differential stability toward different chelator heads were addressed using MBP-H6 and MBP-H10.

Specificity, Activity, and Reversibility. The reactions carried out at high concentration in organic solvents at elevated temperature ensured high coupling efficiency for the protected chelator headgroups. The maximum surface concentration of chelator headgroups was thus determined by the density of terminal amino groups of planar PEG polymer brush, which has been estimated to be ~1/nm^2.[23] The surfaces so obtained were used for studying specificity and reversibility of the interaction with the histidine-tagged proteins as well as the functionality of the immobilized proteins. Both MBP-H10 and ifnar2-H10 readily bound to mono-NTA-functionalized surfaces loaded with nickel(II) ions (Figure

(28) Schuck, P.; Minton, A. P. *Anal. Biochem.* **1996**, *240*, 262−272.
(29) Glaser, R. W. *Anal. Biochem.* **1993**, *213*, 152−161.

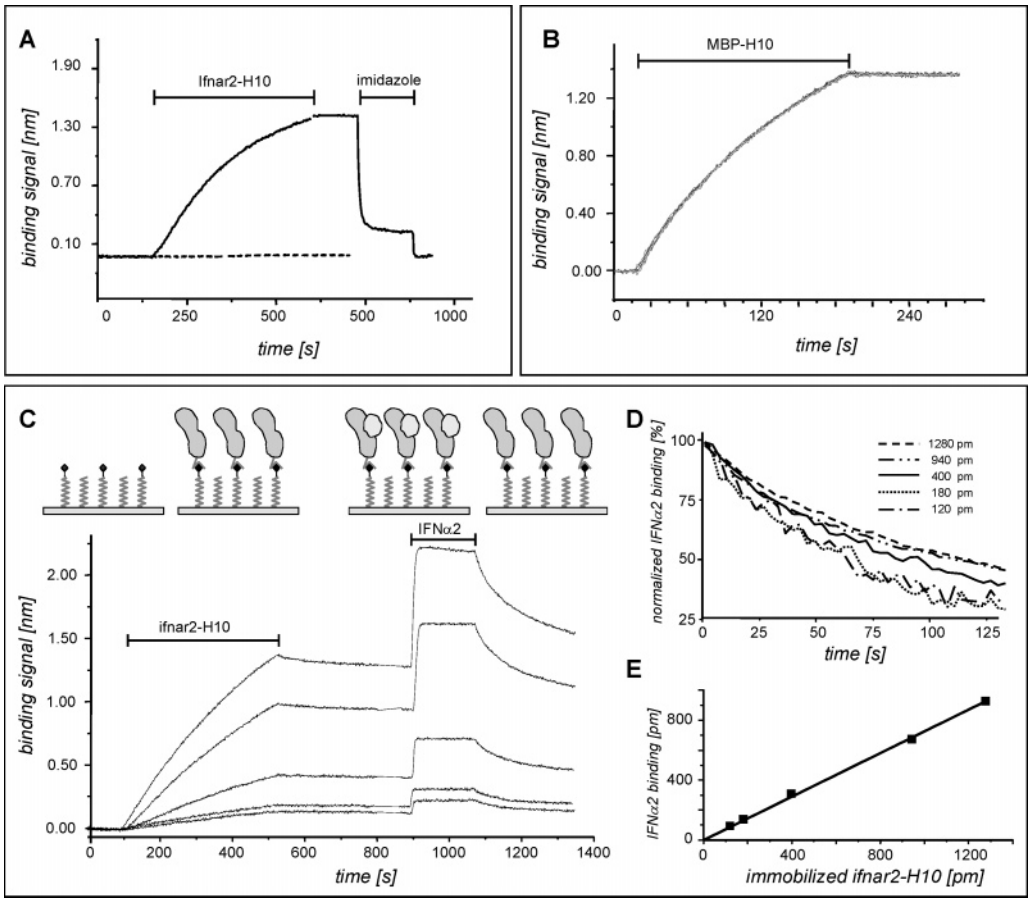

Figure 2. Immobilization on 100% mono-NTA functionalized surfaces: reversibility, specificity, and activity. (A) Binding curve for 400 nM ifnar2-H10 after loading with nickel(II) ions with subsequent elution with 150 mM imidazole (—) and binding of 400 nM ifnar2-H10 after removing nickel(II) ions with EDTA (·····). (B) Overlay plot showing 10 successive immobilization cycles of 250 nM MBP-H10 on 100% mono-NTA functionalized surface upon repeated removal with 150 mM imidazole. (C) Concentration-dependent immobilization of ifnar2-H10 and subsequent binding of 400 nM IFNα2. (D) Normalized dissociation phase of IFNα2 from (C). (E) Maximum IFNα2 binding vs immobilized amplitude of ifnar2-H10.

2A). The protein bound stably and was quantitatively removed with 200 mM imidazole (Figure 2A) or free nickel(II) ions (data not shown). A maximum of ~3.5 and 4.5 ng/mm^2 surface loading was observed at high concentrations of ifnar2-H10 and MBP-H10, respectively (data not shown). These values correspond approximately to a monolayer of these proteins (25 kDa for ifnar2-H10 and 40 kDa for MBP-H10). Significant dissociation was observed at these saturated surface loadings (data not shown). However, the maximum protein loading under these conditions was probably limited by sterical crowding and not by the number of surface binding sites. No deposition above the detection limit of RIfS (10 pg/mm^2) was observed upon removing nickel(II) ions with EDTA (50 mM) from the surface (Figure 2A, dashed line), confirming CMI-specific binding. Furthermore, no binding of nontagged ifnar2-EC as well as MBP onto the nickel(II) loaded mono-NTA surface was detected (data not shown), confirming oligohistidine-tag specific interaction with CMI. To confirm stable nickel(II) ion binding to NTA moieties and reproducible immobilization, MBP-H10 (250 nM) was 10 times sequentially loaded and removed with imidazole (150 mM) from 100% mono-NTA functionalized surface (Figure 2B). No decrease in binding amplitude as a function of loading cycle was observed.

The activity of the immobilized ifnar2-H10 was probed with its ligand IFNα2 at a concentration sufficient to fully saturate the binding sites. In Figure 2C, ifnar2-H10 immobilization on 100% mono-NTA functionalized surface followed by IFNα2 (400 nM) binding is shown. The amount of ifnar2-H10 on the surface was controlled by injecting different concentrations ranging from 25 to 250 nM. IFNα2 deposition increased proportionally to the immobilized amount of ifnar2-H10. This binding was totally specific as, without immobilized ifnar2-H10, mass deposition was below the detection limit (data not shown). The saturation binding amplitude of IFNα2 was plotted as a function of immobilized amount of ifnar2-H10 (Figure 2E). Linear regression gave a slope of 0.72, which is 90% of the expected slope taking the molecular masses of the proteins (~20 kDa for IFNα2, ~25 kDa for ifnar2-H10) into account. Thus, 90% of the immobilized ifnar2-H10 retained its IFNα2 binding activity. The intercept of 6 pM of the fit confirmed negligible nonspecific binding of IFNα2. Shown in Figure 2D is the overlay of the normalized dissociation phase of IFNα2. By fitting eq 1 to the first 100 s the average dissociation rate constant (k_d) was estimated to be 0.010 ± 0.001 s^{-1}. This k_d is in perfect agreement with the k_d observed when ifnar2-EC was immobilized via a monoclonal antibody.[24] In contrast, ifnar2-EC directly adsorbed on glass surfaces did not interact with IFNα2 (data not shown), implying complete denaturation of the protein. Furthermore, when ifnar2-EC was covalently attached via free amines, only ~5% of the bound protein retained activity, and k_d

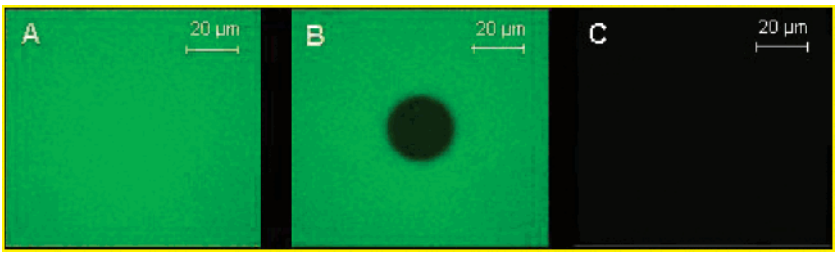

Figure 3. Microscopic homogeneity of the chelator-modified surfaces. (A) Fluorescence image of immobilized MBP-H10 labeled with OG488. (B) Fluorescence image upon bleaching a circular spot of 25 μm in diameter. (C) Fluorescence image upon eluting the protein with 150 mM imidazole.

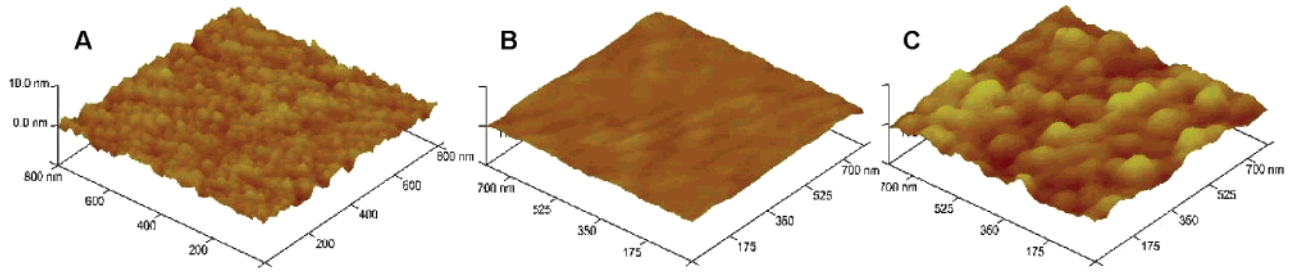

Figure 4. AFM topographical images of modified RIfS transducer surfaces. (A) After cleaning of the surface. (B) After silanization with GOPTS. (C) After covalent coupling of PEG followed by 20% functionalization with bis-NTA.

increased by a factor of 2.[21,24] The same set of experiments was carried out with bis- and tris-NTA modified surfaces. In both the cases, (i) stable immobilization, (ii) complete reversibility of nickel-specific adsorption with imidazole, (iii) reproducible immobilization, and (vi) ≥90% IFNα2 binding activity of immobilized ifnar2-H10 as observed for mono-NTA surfaces was confirmed (data not shown).

Topology and Lateral Homogeneity. The microscopic lateral homogeneity and the nanoscopic topography of the chelator functonalized surface were monitored with CLSM and AFM, respectively. OG488-labeled MBP-H10 was first immobilized on 20% bis-NTA functionalized surface of a coverslip and then imaged with a 63× objective. The surface appeared uniformly fluorescent on 100-μm-length scale indicating uniform immobilization (Figure 3A) To see a contrast, a circular spot with 25-μm diameter was bleached with 100% laser power for ∼7 s (Figure 3B). The immobilized protein was then removed with 150 mM imidazole (Figure 3C). Uniform immobilization and complete removal of the protein with imidazole indicated uniform immobilization with uniform specificity. The topography of the chemically modified silica surfaces was studied with AFM. The RIfS transducers at three different stages of suface modification were imaged in contact mode (Figure 4). The cleaned transducer surfaces (Figure 4A) showed a rms roughness of 0.6 ± 0.2 nm. Upon reaction with GOPTS (Figure 4B), a decrease in rms roughness to 0.3 ± 0.1 nm was observed, indicating healing of surface defects during silanization. A moderate increment to 0.9 ± 0.3 nm rms roughness was observed upon PEG attachment followed by chelator functionalization (Figure 4C).

Affinity and Stoichiometry. Low molecular weight recognition elements such as NTA can be immobilized with much higher surface densities compared to proteins. Such high surface concentration facilitates multipoint attachment and rebinding, thus providing much higher apparent stability compared to an individual interaction.[20] To minimize these biasing effects, the surface concentration of chelator headgroups was substantially decreased compared to the maximum by partially blocking the terminal functional groups of the PEG layer prior to coupling the chelator headgroups (**1**, **2**) or by reducing the coupling time to a few minutes (**3**). The interaction of different oligohistidine tags with different chelator heads was studied using these rarely functionalized surfaces. Full saturation of the binding sites was ensured by injecting the proteins at high concentrations up to 50 μM. Control experiments without loading the nickel(II) ensured that no significant nonspecific binding and background signal were observed under these conditions (data not shown). In all the cases, the saturation binding amplitudes for MBP were typically 2−3 nm, implying an average distance between the binding sites ranged between 5 and 7 nm. Figure 5A shows the binding curves for MBP-H10 and MBP-H6 when injected on a 20% mono-NTA functionalized surface. For both the proteins, fast dissociation during the first 100 s was observed, which afterward slowed without reaching the baseline: after 400 s of rinsing, more than 15% of MBP-H6 and ∼50% of MBP-H10 remained on the surface, suggesting that the protein was entrapped by rebinding and multipoint attachment. For the initial, fast dissociation phase, (apparent) dissociation rate constants of 0.3 ± 0.05 s^{-1} for MBP-H6 and 0.03 ± 0.005 s^{-1} for MBP-H10 were determined. Thus, the additional four histidines stabilized binding by 1 order of magnitude, corroborating the key role of multipoint attachment and rebinding for the observed binding stability. Irreversible binding as observed at the higher mono-NTA surface concentration (cf. Figure 2) is, therefore, not achieved by stable, stoichiometric interaction, but probably by more efficient multipoint attachment. The interaction of MBP-H6 and MBP-H10 with nickel(II)-loaded bis- and tris-NTA was measured under the same conditions, i.e., saturation of rarely functionalized surface. A comparison of the normalized dissociation phase of MBP-H10 from mono and multivalent chelator heads is shown in Figure 5B. In contrast to mono-NTA, no dissociation of the H10-tagged protein

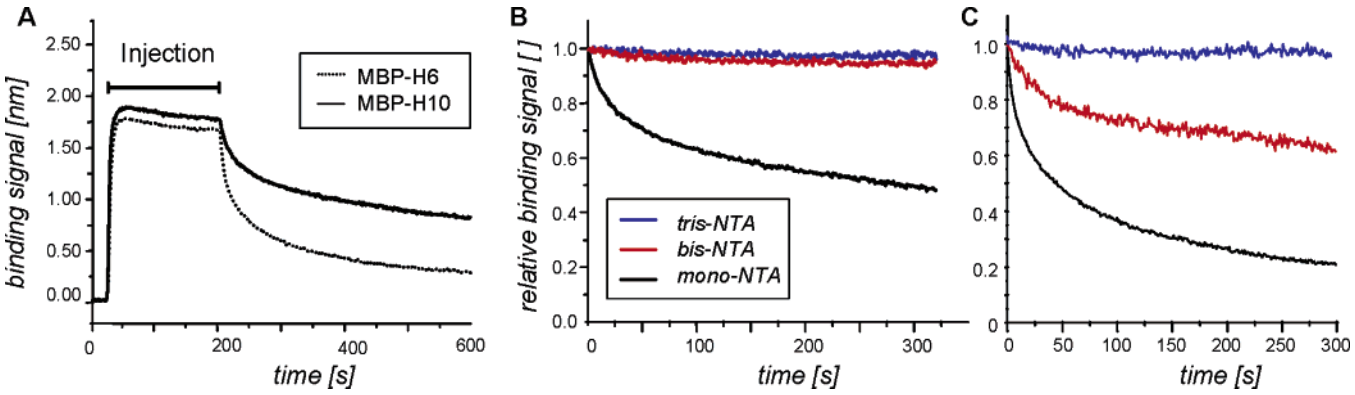

Figure 5. Binding stability at reduced chelator surface concentration. (A) Binding curves for 50 μM MBP-H10 and MBP-H6 on a mono-NTA functionalized surface. (B, C) Comparison of the dissociation phases of MBP−H10 (B) and MBP-H6 (C) from mono-NTA, bis-NTA, and tris-NTA functionalized surfaces.

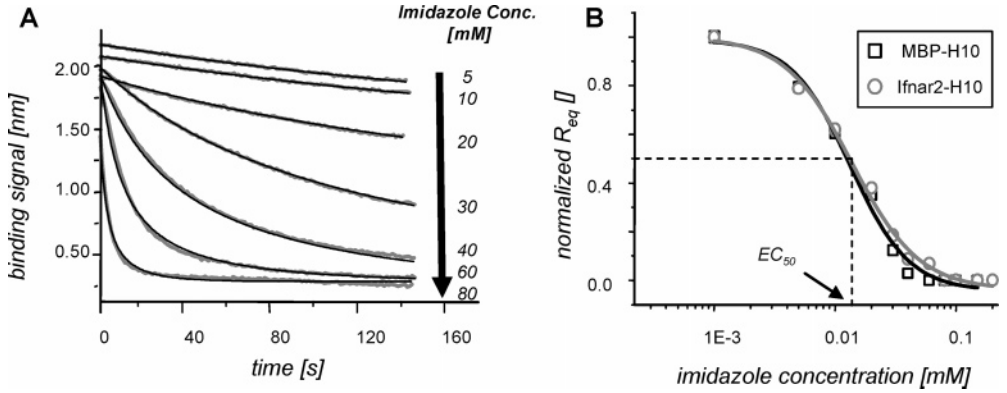

Figure 6. Imidazole-induced dissociation on mono-NTA functionalized PEG layers. (A) Overlay of the dissociation phases at different imidazole concentrations (gray lines) and fit of eq 4 (black lines) for MBP-H10. (B) Normalized $R_{trapped}$ vs imidazole concentration for MBP-H10 and ifnar2-H10.

from tris-NTA and bis-NTA was detectable. For MBP-H6, significant dissociation (~30% of the total amplitude) was observed also from bis-NTA with an initial k_d of 0.02 ± 0.005 s^{-1} (Figure 5C). Binding of MBP-H6 to tris-NTA, however, was still entirely stable. These results demonstrate the increase in binding stability with increasing multivalency. Strikingly, stoichiometric and stable immobilization of proteins with a single H6 tag was achieved with tris-NTA, independent of its surface concentration.

Imidazole-Induced Dissociation. MBP-H10 bound to tris-NTA and bis-NTA in a stable manner, and the relative stability could not be determined directly. To assess the difference among stable binding pairs, dissociation was induced with imidazole. The dissociation phase of ifnar2-H10 immobilized on a 100% mono-NTA functionalized surface is shown in Figure 6A for different imidazole concentrations ranging from 5 to 80 mM. Again eq 1 could not be fitted to the dissociation phase without large systematic errors. Using residual binding as a diagnostic for rebinding and multipoint attachment, eq 3 was fitted to determine $R_{trapped}$, which turned out to be the most robust parameter for comparing different experiments. Imidazole concentration-dependent dissociation phases and the corresponding fits are shown in Figure 6A. The $R_{trapped}$ determined from these fits was plotted as a function of imidazole concentration (Figure 6B). A characteristic transition of $R_{trapped}$ from 100 to 0% between 1 and 80 mM imidazole was observed, which was fitted to a logistic sigmoidal function (eq 4). The imidazole concentration at the inflection point of the sigmoidal curve, i.e., elution concentration for 50% $R_{trapped}$ (EC_{50}), is the characteristic concentration for a given interaction: the more stable the interaction the higher competitor concentration is required to disrupt it. The steepness of the curve is quantified by the parameter p of eq 4. For MBP-H10 and mono-NTA functionalized surface EC_{50} was estimated to be 13.5 mM. The dependence of $R_{trapped}$ on the imidazole concentration for ifnar2-H10 and MBP-H10 is shown for comparison in Figure 6B. The overlaying curves (i.e., same EC_{50} and p) observed for these identically tagged, different monomeric proteins suggest that the assay is unbiased by the nature of the protein. The same assay was carried out for bis- and tris-NTA as well (Figure 7A). The EC_{50} increased in the following order, mono-NTA < bis-NTA < tris-NTA, confirming the increase in stability with the number of coordination sites (Figure 7A). Interestingly, an increment in the steepness, i.e., p, with increasing multivalency of the chelator heads was observed (Table 1.). Since the cause of $R_{trapped}$ is rebinding and multipoint attachment, increasing steepness of the curves with increasing EC_{50} suggests relatively minor contribution of these undefined heterogeneous effects over molecularly defined stability of a given interaction. For tris-NTA, the same analysis was carried out with MBP-H6 (Figure 7B). A large 6-fold decrease in the EC_{50} in comparison to MBP-H10 was observed. The steep, surface concentration-invariant titration curves suggest that discrimination between H6- and H10-tagged proteins is possible by using 30 mM imidazole as a selectivity filter (Figure 7B). Since for mono- and bis-NTA no stable attachment of H6-tagged proteins was observed, imidazole-induced dissociation was not investigated.

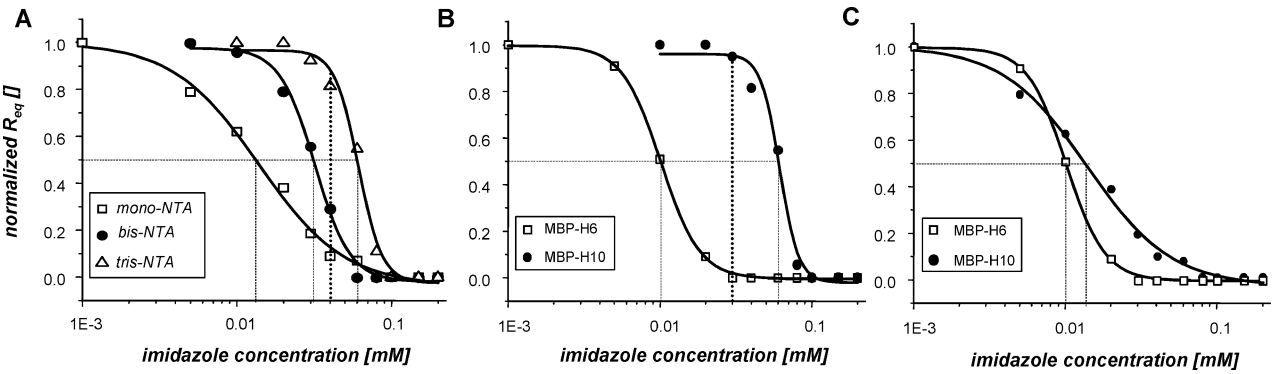

Figure 7. (A) Normalized $R_{trapped}$ as a function of imidazole concentration for MBP-H10 on mono-NTA, bis-NTA, and tris-NTA functionalized surfaces. (B) Normalized $R_{trapped}$ as a function of imidazole concentration for MBP-H10 and MBP-H6 on tris-NTA functionalized surface. Dashed lines indicate the EC_{50}, and dotted lines indicate the imidazole concentration for optimum selectivity. (C) Comparison of MBP-H10/mono-NTA and MBP-H6/tris-NTA.

Table 1. EC_{50} and *p*-Values from Imidazole-Induced Dissociation Experiments with MBP-H10 and MBP-H6 from Surfaces Functionalized with different Chelator Heads[a]

	EC_{50} (H10) (mM)	*p* (H10)	EC_{50} (H6) (mM)	*p* (H6)
mono-NTA	13.8 ± 0.001	1.6 ± 0.2	nd[b]	nd
bis-NTA	31.9 ± 0.001	3.8 ± 0.5	nd	nd
tris-NTA	61.0 ± 0.002	5.7 ± 1.2	10.2 ± 0.002	3.3 ± 0.2

[a] The errors were estimated from the fit. [b] nd, not determined because stability was too low for the assay.

Figure 7C shows a comparison of the titration curves obtained for the interaction of MBP-H6 with tris-NTA and MBP-H10 with mono-NTA. These interaction pairs show a very similar EC_{50} of 10.2 and 13.5 mM, respectively. Strikingly, however, the steepness of the curve (i.e., the *p*-value, cf. Table 1) is considerably higher in case of MBP-H6/tris-NTA compared to MBP-H10/mono-NTA, yet again pointing at molecularly defined immobilization by multivalent interaction between H6 and tris-NTA.

Blocking Excess CMI. For applications of solid-phase detection formats for probing biomolecular interactions, nonspecific interactions between the analyte and the surface is an extremely critical issue. Since the side chains of the natural amino acids often carry potential metal coordinating groups (Cys, Lys, Glu, Asp, Trp, His), metal ion binding is often an intrinsic property of many proteins and a serious limitation for CMI immobilization strategy. Furthermore, high excess of the negatively charged CMI changes the electrostatic properties of the surface and thus affects the interaction with charged proteins. The interaction between IFNβ and covalently immobilized ifnar2-EC could not be measured on a dextran surface under physiological conditions (150 mM NaCl; pH 7.5) due to high nonspecific adsorption of positively charged IFNβ on negatively charged extended dextran hydrogel.[21,30] Additionally, IFNβ has a metal ion binding site, making interaction analysis on a CMI-loaded surface even more challenging. The binding of IFNβ with and without immobilized ifnar2-H10 on 100% mono-NTA functionalized PEG layers is shown in Figure 8A. Owing to high surface concentration of chelator heads (necessary for stable immobilization of H10-tagged proteins), substantial metal ion specific adsorption of IFNβ (Figure 8A) was observed (1.2 nm) even without immobilized ifnar2-H10. Though the adsorption of IFNβ increased upon ifnar2-H10 immobilization, deconvolution of ifnar2-H10-specific affinity and kinetic characteristics was not possible. IFNβ bound to rarely (10−20%) tris-NTA functionalized layers as well (Figure 8B) but to a much lower extent (0.15 nm). After blocking the binding sites with MBP-H10, no adsorption was observed (Figure 8B). For studying the interaction of IFNβ with ifnar2-H10, ifnar2-H10 was immobilized and excessive binding sites were then blocked with MBP-H10. Binding of IFNβ is shown in Figure 8B (solid trace). Compared to the constantly increasing binding curves shown in Figure 8A, saturation was reached very fast as observed also for IFNα2 (cf. Figure 2C). The signal amplitude corresponded stoichiometrically to the amount of immobilized ifnar2-EC, corroborating that entirely specific interaction was detected. Furthermore, the same experiment was performed with ^{I47A}ifnar2-H10 as well (Figure 8B, dashed−dotted trace). As reported earlier,[30] IFNβ dissociated faster from this mutant than from wild-type ifnar2-H10. This example demonstrates two distinct advantages of high-affinity MCH versus mono-NTA to overcome nonspecific binding: (i) stable immobilization can be obtained already at low CH surface concentration, thus reducing the number of excess CMI on the surface; (ii) remaining excess CMI can be efficiently blocked with an indifferent H10-tagged protein to further minimize nonspecific adsorption.

Blocking Oligohistidine Tags in Solution. The oligohistidine tag is frequently used for protein purification: often not only the immobilized protein but also the interaction partner in solution carries an oligohistidine tag. Under these conditions, immobilization by CMI is critical as the interaction partner in solution simultaneously interacts with both the excess CMI and the immobilized protein. Given the stoichiometric, high-affinity interaction between the tag and the chelator head, carrying out interaction analysis with a soluble histidine-tagged protein by blocking the excess CMI on the surface or by blocking the tag with the soluble chelator head should be feasible. We tested out this possibility for tris-NTA functionalized surfaces by immobilizing ifnar1-H10 and carrying out the interaction analysis with ^{mut}IFNα2 in complex with soluble ifnar2-H6. Binding of histidine-tagged

(30) Piehler, J.; Schreiber, G. *J. Mol. Biol.* **1999**, *294*, 223−237.

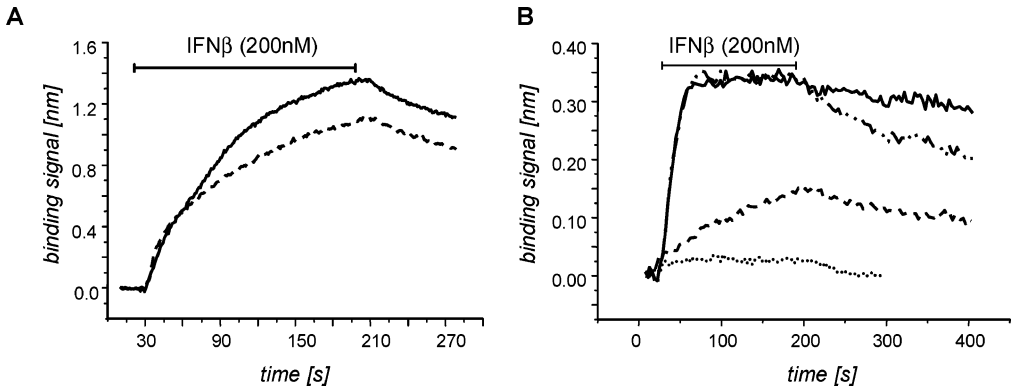

Figure 8. Blocking of excess CMI on the surface. (A) IFNβ binding on a 100% mono-NTA-functionalized surface with (—) and without (···) immobilized ifnar2-H10. (B) IFNβ binding on rarely tris-NTA functionalized surface before (– –) and after (···) blocking with MBsP-H10 and upon immobilization of ifnar2-H10 (—) or ^{I47A}ifnar2-H10 (—··—) followed by blocking with MBP-H10.

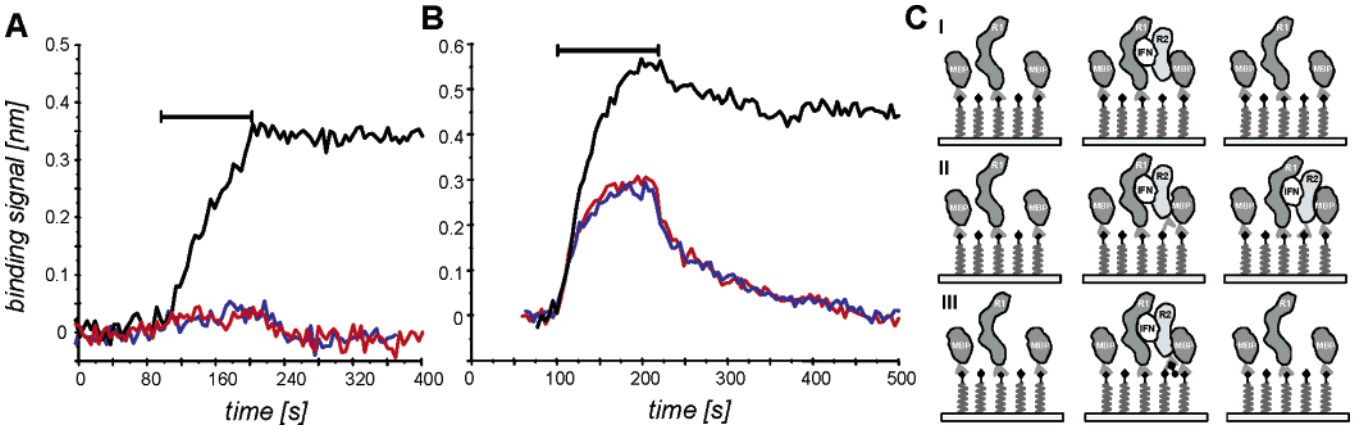

Figure 9. Blocking of the H6-tag in solution. (A) Signals observed for 100 nM ifnar2-H6 before (black) and after (blue) immobilization of ifnar1-H10 and blocking with MBP-H10; in comparison, the signal for 100 nM ifnar2-H6 in the presence of 150 nM Ni^{2+}-loaded tris-NTA on the CMI-loaded surface without immobilized protein is shown (red). (B) Binding of 100 nM ^{mut}IFNα2 in stoichiometric complex with ifnar2-H6 (black), with ifnar2-EC (blue), and with ifnar2-H6 in the presence of 150 nM Ni^{2+}-loaded tris-NTA (red) to ifnar1-H10 immobilized on tris-NTA functionalized surface. The surface was blocked with 1 μM MPB-H10 for all experiments. (C) Schematic of the binding experiments with immobilized ifnar1-H10 (R1) as shown in (B). Binding and dissociation of ^{mut}IFNα2 in complex with ifnar2-EC (R2) (I, blue curve in B), with ifnar2-H6 (II, black curve in B) and with ifnar2-H6 and stoichiometric amounts of Ni^{2+}-loaded tris-NTA (III, red curve in B).

proteins to Ni^{2+}-loaded tris-NTA surface was efficiently blocked after saturating the surface with MBP-H10 (Figure 9A). Alternatively, binding of ifnar2-H6 could also be blocked by adding a 1.5-fold excess of soluble, CMI-loaded tris-NTA in solution (Figure 9A). Blocking of CMI on the surface by MBP-H10, however, was insufficient when the tagged protein specifically interacted with the immobilized receptor (Figure 9B): while IFNα2 in complex with ifnar2-EC dissociated from immobilized ifnar1-H10 with a rate constant of 0.02 s^{-1}, no dissociation and a higher binding amplitude was observed for the complex with ifnar2-H6. Probably CMI sites buried by the proteins on the surface could still be recruited by the H6-tagged protein, which was strongly enriched at the surface by the specific interaction with the immobilized protein. In the presence of a 1.5-fold molar excess of Ni^{2+}-loaded tris-NTA in solution, however, the interaction curve perfectly overlaid with the trace for tagless ifnar2-EC. Thus, unbiased interaction with a H6-tagged protein could be measured due to successful masking of the H6-tag by tris-NTA in solution.

CONCLUSIONS

We attempted to design a surface architecture for functional protein immobilization on glass-type surfaces, which is generally compatible with solid-phase detection techniques. Ultrathin, dense PEG layers attached covalently onto glass-type surfaces effectively precluded nonspecific interaction and denaturation of immobilized proteins, while maintaining a flat, two-dimensional arrangement of the recognition sites for protein tethering close to the transducer interface. Stable, yet reversible tethering of proteins to this surface in an oriented fashion was achieved by employing MCH engineered for high-affinity recognition of oligohistidine tags. In this way, high surface concentration and stoichiometric excess of CMI, which are required for immobilization via mono-NTA, were avoided. Based on biologically representative ligand–receptor interactions, we demonstrated some key advantages of these MC—in particular tris-NTA—compared to the traditional mono-NTA: (i) high-affinity tethering independent of the surface concentration; (ii) minimal nonspecific adsorption due to low MCH

surface concentration and blocking of excess CMI with an indifferent oligohistidine-tagged protein; (iii) unbiased biomolecular interaction measurements with histidine-tagged proteins by blocking the histidine tag with soluble MCH; (iv) potential, molecularly defined selectivity of MCH toward different oligohistidine tags. The chemical nature of these high-affinity recognition units furthermore ensures well-defined surface architecture and long-term stability in comparison to protein-based affinity systems. Coupling of the MCH onto a thin, flat PEG polymer brush turned out to be highly useful for analyzing the function of immobilized proteins. Thus, immobilization of the extracellular domain of the type I interferon receptor, ifnar2-EC, was possible up to surface concentrations of more than 20% of a monolayer, while retaining 90% functional. The simple bottom-up surface chemistry can be used for all glass-type substrates. The unique properties of the surfaces in terms of biocompatibility and oriented, stable protein attachment make them attractive for bioanalytical and biophysical applications including label-free and fluorescence detection, as well as scanning probe techniques. Furthermore, functional surface patterning using MCH with different affinities and its application for protein arrays can be envisaged.

ACKNOWLEDGMENT

IFNβ (Rebif) was kindly provided from Dr. Garth Virgin, Serono GmbH, Unterschleissheim. This work was supported by the DFG (Pi-405/1, Pi-405/2-1) and by the BMBF (0312005A). We thank Gerhardt Spatz-Kümbel, Martynas Gavutis, and Annett Reichel for excellent experimental support, as well as Peter Lamken and Eva Jaks for providing proteins. The hospitality and the support from the laboratory of Robert Tampé are gratefully acknowledged, in particular Karin Busch and Ali Tinazli for their help with CLSM and AFM measurements, respectively, and for helpful discussions. We thank the reviewers for their encouraging and helpful comments.

Received for review August 11, 2004. Accepted November 15, 2004.

AC048813J